Lipid raft–dependent plasma membrane repair interferes with the activation of B lymphocytes

Heather Miller, Thiago Castro-Gomes, Matthias Corrotte, Christina Tam, Timothy K. Maugel, Norma W. Andrews, and Wenxia Song

Department of Cell Biology and Molecular Genetics, University of Maryland, College Park, MD 20742

Cells rapidly repair plasma membrane (PM) damage by a process requiring Ca^{2+}-dependent lysosome exocytosis. Acid sphingomyelinase (ASM) released from lysosomes induces endocytosis of injured membrane through caveolae, membrane invaginations from lipid rafts. How B lymphocytes, lacking any known form of caveolin, repair membrane injury is unknown. Here we show that B lymphocytes repair PM wounds in a Ca^{2+}-dependent manner. Wounding induces lysosome exocytosis and endocytosis of dextran and the raft-binding cholera toxin subunit B (CTB). Resealing is reduced by ASM inhibitors and ASM deficiency and enhanced or restored by extracellular exposure to sphingomyelinase. B cell activation via B cell receptors (BCRs), a process requiring lipid rafts, interferes with PM repair. Conversely, wounding inhibits BCR signaling and internalization by disrupting BCR–lipid raft coclustering and by inducing the endocytosis of raft-bound CTB separately from BCR into tubular invaginations. Thus, PM repair and B cell activation interfere with one another because of competition for lipid rafts, revealing how frequent membrane injury and repair can impair B lymphocyte–mediated immune responses.

Introduction

Plasma membrane (PM) wounding can occur during the lifetime of most cells, caused either by external mechanical forces (McNeil and Ito, 1989, 1990), pore-forming proteins secreted by pathogens (Los et al., 2013), or internal forces generated by contraction and/or migration (Chen, 1981; McNeil and Khakee, 1992; Clarke et al., 1995). To avoid lethal events triggered by massive Ca^{2+} influx and cytosol depletion (Geeraerts et al., 1991), eukaryotic cells rapidly repair PM wounds. The importance of PM repair has been shown in muscle fibers, which are frequently injured during contraction. Failure in resealing of the muscle sarcolemma has been identified as a cause of muscular dystrophy (Bansal et al., 2003).

Early studies discovered that PM repair is triggered by Ca^{2+} influx through wounds in the PM (Steinhardt et al., 1994; Andrews et al., 2014). Ca^{2+} influx induces lysosome exocytosis, which exposes lysosomal membrane proteins on the cell surface and releases lysosomal contents (Reddy et al., 2001; Jaiswal et al., 2002; Tam et al., 2010). Exposure of the lumenal domain of the lysosomal-associated membrane protein 1 and the lysosomal synaptotagmin isoform Syt VII are detected a few seconds after wounding, reflecting the rapid Ca^{2+}-dependent fusion of lysosomes with the PM (Reddy et al., 2001). Exocytosed lysosomes were initially suggested to provide the membrane needed for resealing, working as a patch to repair open wounds. More recently, it became evident that lysosomal exocytosis is followed by a rapid form of endocytosis that can remove lesions from the PM (Idone et al., 2008; Tam et al., 2010; Corrotte et al., 2012).

Recent studies revealed that PM wounding by the pore-forming toxin streptolysin O (SLO) or by mechanical forces triggers endocytosis of caveolae (Corrotte et al., 2013), PM invaginations that are localized in lipid rafts (Galbiati et al., 2001). Evidence supporting this finding includes the colocalization of caveolin and SLO in <80 nm intracellular vesicles, accumulation of intracellular vesicles with morphological characteristics of caveolae (<80-nm-diameter flask-shaped and uncoated vesicles; Parton and Simons, 2007) at wound sites in cell lines and primary muscle fibers, and inhibitory effects of caveolin deficiency on PM repair (Gazzerro et al., 2010; Corrotte et al., 2013). The involvement of caveolae in the endocytosis-mediated PM repair process is also consistent with the severe muscle pathology that is observed in mice deficient in caveolin and other caveolae-associated proteins such as cavin (Hagiwara et al., 2000; Hnasko and Lisanti, 2003).

Caveolin-mediated endocytosis of injured PM can be induced by exposure to acid sphingomyelinase (ASM; Tam et al., 2010; Corrotte et al., 2013). Via Ca^{2+}-dependent lysosome exocytosis, ASM is released to the outer leaflet of the PM, where it generates ceramide from sphingomyelin (Grassmé et al., 2002; Xu et al., 2012). Ceramide was proposed to induce

Correspondence to Wenxia Song: wenxsong@umd.edu

Abbreviations used in this paper: AF, Alexa Fluor; ASM, acid sphingomyelinase; BCR, B cell receptor; CTB, cholera toxin B subunit; DPA, desipramine; LIMP, lysosomal integral membrane protein; MFI, mean fluorescence intensity; PE, phycoerythrin; PI, propidium iodide; PM, plasma membrane; SLO, streptolysin O; SM, sphingomyelinase; TEM, transmission electron microscopy.

The Rockefeller University Press $30.00
J. Cell Biol. Vol. 211 No. 6 1193–1205
www.jcb.org/cgi/doi/10.1083/jcb.201505030

caveolae-mediated endocytosis by creating membrane curvature and facilitating the recruitment of caveolin to lipid rafts (Andrews et al., 2014). The importance of ASM in PM repair has been demonstrated by the finding that extracellular exposure to ASM restores membrane resealing even in the absence of extracellular Ca^{2+} (Tam et al., 2013). Moreover, inhibition or depletion of ASM reduces wounding-induced endocytosis and PM resealing (Tam et al., 2010). Thus, increasing evidence supports a closely coordinated process of Ca^{2+}-induced lysosome exocytosis and ASM-dependent caveolin-mediated endocytosis as an important mechanism for PM repair. However, it is not known if this form of PM repair is universal or if different cell types that express distinct regulatory proteins use distinct mechanisms to reseal after injury.

B lymphocytes are circulating cells that attach to substrates and migrate in response to stimuli (Brandes et al., 2000; Pereira et al., 2010). After maturation in the bone marrow, B cells circulate through the body to survey for the presence of pathogenic substances. In response to pathogen signals, B cells extravasate, migrating through endothelial cells to reach infected sites. B cells also migrate through dense and well-organized lymphoid tissues, the spleen and lymph nodes, where they capture and present antigen and mount responses (Okada et al., 2005; Batista and Harwood, 2009). B cells extract antigen from antigen-presenting cells, internalize and process antigen in late endosomes, and present antigen in complexes with major histocompatibility complex class II for T cell recognition (Okada et al., 2005; Yuseff et al., 2013). Through these processes, B cells face ample possibilities of wounding their PM. However, unlike epithelial cells, fibroblasts, and myofibers, which have been well studied regarding their PM repair ability, nothing is known about how B cells cope with injury. Different from those well studied cells as well as T lymphocytes (Tomassian et al., 2011), B lymphocytes do not contain detectable levels of known isoforms of caveolin (Fra et al., 1994), even though B cells may express caveolin during in vitro differentiation into plasma cells (Medina et al., 2006). Despite the apparent lack of caveolin, the organization of signalosomes and the endocytic machinery in B cells is highly dependent on lipid rafts (Cheng et al., 1999, 2001; Stoddart et al., 2002), cholesterol and sphingolipid-rich PM domains where caveolin normally resides (Galbiati et al., 2001). B cell activation is induced by the B cell receptor (BCR). Upon antigen binding, surface BCRs oligomerize into microclusters in lipid rafts, where the cytoplasmic tails of the receptor are phosphorylated by raft-resident Src kinases in the inner leaflet of the PM. Phosphorylated cytoplasmic domains of the BCR recruit and activate downstream signaling molecules, propagating signaling cascades (Pierce, 2002; Dal Porto et al., 2004). Lipid rafts are also essential for BCR internalization, by which B cells capture antigen for processing (Stoddart et al., 2005; Bléry et al., 2006). We and others have demonstrated that lipid rafts act to couple BCR signaling and endocytosis by recruiting endocytic machinery to the vicinity of signalosomes (Stoddart et al., 2002). The unique properties of B lymphocytes, the importance of lipid rafts in their immunological functions, and the fact that injury is likely to occur as these cells migrate in vivo raise the question of whether and how B lymphocytes repair PM wounds.

In this study, we show that primary B lymphocytes can effectively repair membrane wounds in the absence of caveolin. The membrane repair process depends on Ca^{2+} influx, Ca^{2+}-induced lysosome exocytosis, and lipid raft–mediated, clathrin-independent endocytosis. Our results reveal that the PM repair mechanism inhibits the signaling and antigen internalization functions of the BCR, probably by interfering with access of the receptor to lipid rafts.

Results

Primary mouse B cells repair PM wounds in a Ca^{2+}-dependent manner

To determine whether B cells are capable of repairing PM wounds, primary B cells freshly isolated from mouse spleens were incubated with increasing concentrations of SLO (0 to ∼400 ng/ml) with or without Ca^{2+} in the culture medium. SLO is a bacterial toxin that binds to cholesterol in membranes and oligomerizes into pores, thus permeabilizing the PM. The membrane impermeant dye propidium iodide (PI) was used to stain B cells that were injured and did not reseal at 5 min after SLO exposure. The percentage of PI^+ cells was quantified by flow cytometry. In the absence of SLO, only small percentages of cells were PI^+ in the presence or absence of extracellular Ca^{2+} (Fig. 1 A), reflecting the spontaneous apoptosis known to occur gradually in primary mouse B cells in the absence of stimuli (Rothstein, 1996; Wurster et al., 2002). In the absence of Ca^{2+}, the percentage of PI^+ B cells increased with the concentration of SLO, reaching a plateau at 200 ng/ml (Fig. 1, A and B). In the presence of Ca^{2+}, the percentage of SLO-treated PI^+ cells was reduced to ∼30% from ∼70% of B cells treated with SLO in the absence of Ca^{2+} when the SLO concentration was 200 ng/ml, indicating that almost half of SLO-damaged cells resealed under these conditions (Fig. 1, B and C). As expected, even in the presence of Ca^{2+}, the percentage of PI^+ cells increased with the concentration of SLO, showing a reduced resealing capacity of B cells as the SLO concentration rose (Fig. 1, B and C). These results indicate that primary mouse B cells are capable of repairing PM wounds caused by SLO and that PM repair in B cells is a Ca^{2+}-dependent process.

Wounding-induced lysosomal exocytosis is involved in B cell PM repair

Cell wounding induces lysosomal exocytosis, and ASM released from lysosomes is required for PM repair in epithelial cells, fibroblasts, and myofibers (Tam et al., 2010; Corrotte et al., 2013). In contrast to these types of cells, resting primary lymphocytes are significantly smaller and thought to have fewer lysosomes and limited volumes of cytoplasm per cell (Monroe and Cambier, 1983; Hat et al., 2011). This raises the question of whether wounding the PM of primary lymphocytes induces lysosome exocytosis and whether lysosome exocytosis is important for PM repair in these cells. We analyzed lysosomal exocytosis in SLO-wounded primary B cells by surface detection of the lysosomal membrane protein LIMP2 and release of the lysosomal enzymes ASM and β-hexosaminidase (β-hex) into the medium. Surface LIMP2 was detected using an antibody specific for the lumenal domain of the protein by both immunofluorescence microscopy and flow cytometry without permeabilizing the cells. Immunofluorescence microscopic analysis found that under the permeabilization condition, LIMP2 staining appeared as puncta in the cytoplasm but not on the PM of SLO-untreated cells, identified by surface BCR labeling (Fig. 2 A). After 5 min of SLO treatment, LIMP2 become detectable at the cell surface (Fig. 2 A). Flow cytometry analysis quantitatively confirmed the immunofluorescence microscopy results (Fig. 2 B). ASM

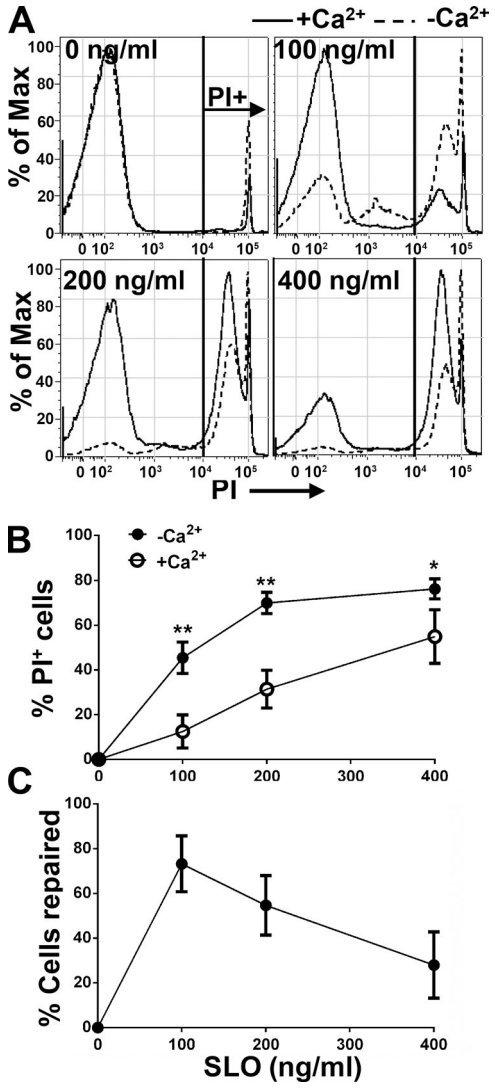

Figure 1. **Mouse primary B cells repair SLO-induced plasma membrane wounds in a Ca^{2+}-dependent manner.** Primary mouse B cells were incubated with SLO (0–400 ng/ml) at 4°C for 5 min and warmed up to 37°C for 5 min in medium with ($+Ca^{2+}$) or without Ca^{2+} ($-Ca^{2+}$), followed by PI staining at 4°C. The percentage of PI positive (PI^+) cells was quantified as nonrepaired cells using flow cytometry (A) and normalized to untreated cells (B). The percentage of cells repaired was calculated as: [$\%PI^+$ ($-Ca^{2+}$) − $\%PI^+$ ($+Ca^{2+}$)] × 100/$\%PI^+$ ($-Ca^{2+}$; C). Shown are representative histograms (A) and the mean (± SD; B and C) of three independent experiments. *, $P < 0.05$; **, $P \leq 0.0005$.

secretion was analyzed by measuring its enzymatic activity and the amount of protein released into the supernatant of the B cell cultures. The level of ASM activity in the supernatant of B cells treated with SLO was significantly higher than that of untreated B cells (Fig. 2 C). Consistently, there was a much higher level of ASM protein in the supernatant of B cells injured by SLO than that in untreated B cells (Fig. 2 D). To determine the fraction of cellular lysosomal enzymes exocytosed upon PM wounding, we quantified the percentage of β-hex secreted by measuring its enzymatic activity in the lysate of untreated cells (total) and in the supernatant of SLO-treated cells (secreted). We found that the percentage of secreted β-hex was significantly increased in SLO-treated cells compared with that in SLO-untreated cells (Fig. 2 E). The results from the three different approaches all indicate that injury of the B cell PM induces lysosome exocytosis.

To determine whether injury-induced release of active ASM is required for B cells to repair their PM, we inhibited ASM with desipramine (DPA; Kölzer et al., 2004) or used primary B cells from ASM knockout mice (Horinouchi et al., 1995). DPA treatment reduced the ability of B cells to repair their PM by 50% (Fig. 2 F), the same percentage of inhibition previously observed in SLO-wounded NRK cells (Tam et al., 2010). Similarly, B cells from ASM knockout mice showed ∼35% reduction in PM repair (Fig. 2 G). Because the later results could have been a consequence of compensatory mechanisms developed in ASM knockout mice, we investigated whether addition of purified sphingomyelinase (SM) extracellularly, mimicking ASM secretion, was able to restore the capability of B cells to repair PM wounds, when the process is reduced by ASM knockout or blocked by a lack of extracellular Ca^{2+}. Indeed, extracellular SM restored the efficacy of ASM knockout B cells to repair their PM wounds to the level of wild-type B cells (Fig. 2 G). Importantly, incubation of SLO-treated B cells with SM in the absence of Ca^{2+} significantly increased the percentage of B cells that fully resealed their PM, compared with no-SM controls (Fig. 2 H). These data suggest that PM repair in B cells requires ASM released by lysosomal exocytosis.

B cell injury by SLO induces ASM-dependent endocytosis of lipid raft–bound cholera toxin subunit B

Endocytosis of caveolae was shown to be involved in the repair of PM wounds in fibroblasts and muscle fibers (Corrotte et al., 2013). To determine whether wounding the PM of B cells, which do not express any known forms of caveolin, also induces endocytosis, we used Texas red–dextran to follow nonspecific fluid-phase uptake and cholera toxin subunit B (CTB) to monitor lipid raft–dependent endocytosis. CTB binds glycosphingolipid GM1, which is enriched in lipid rafts, the same membrane domain from where caveolae-mediated endocytosis normally occurs. Immunofluorescence microscopic analysis showed that in Ca^{2+}-free medium dextran entered the cytosol and diffused throughout SLO-treated cells, indicating that these cells were permeable, and their PM was not repaired (Fig. 3 A, top). In the presence of Ca^{2+}, dextran was almost undetectable within SLO-untreated cells (Fig. 3 A, middle) but appeared punctate in the periphery of SLO-treated cells, consistent with endocytosis (Fig. 3 A, bottom). The percentage of B cells showing dextran endocytosis was significantly increased after 5-min exposure to SLO, when compared with untreated B cells (Fig. 3 B). This result indicates that PM wounding triggers rapid endocytosis of dextran by B cells. To determine whether the dextran endocytosis induced by SLO is dependent on ASM released by lysosomal exocytosis, we examined the effect of extracellular treatment with SM on dextran endocytosis in the absence of SLO. We found that SM treatment alone induced dextran endocytosis to a level similar to SLO treatment in the presence of Ca^{2+} (Fig. 3 B). These results suggest the rapid fluid phase endocytosis triggered by wounding in B cells is ASM dependent.

The endocytosis of CTB was analyzed by immunofluorescence microscopy, flow cytometry, and transmission immunoelectron microscopy (TEM). Immunofluorescence microscopic analysis found that surface-labeled CTB became colocalized with intracellular dextran puncta in SLO-treated cells but remained at the PM in SLO-untreated cells (Fig. 3, A and C), suggesting that CTB and dextran enter cells together in response to SLO treatment. Using flow cytometry, we quantified

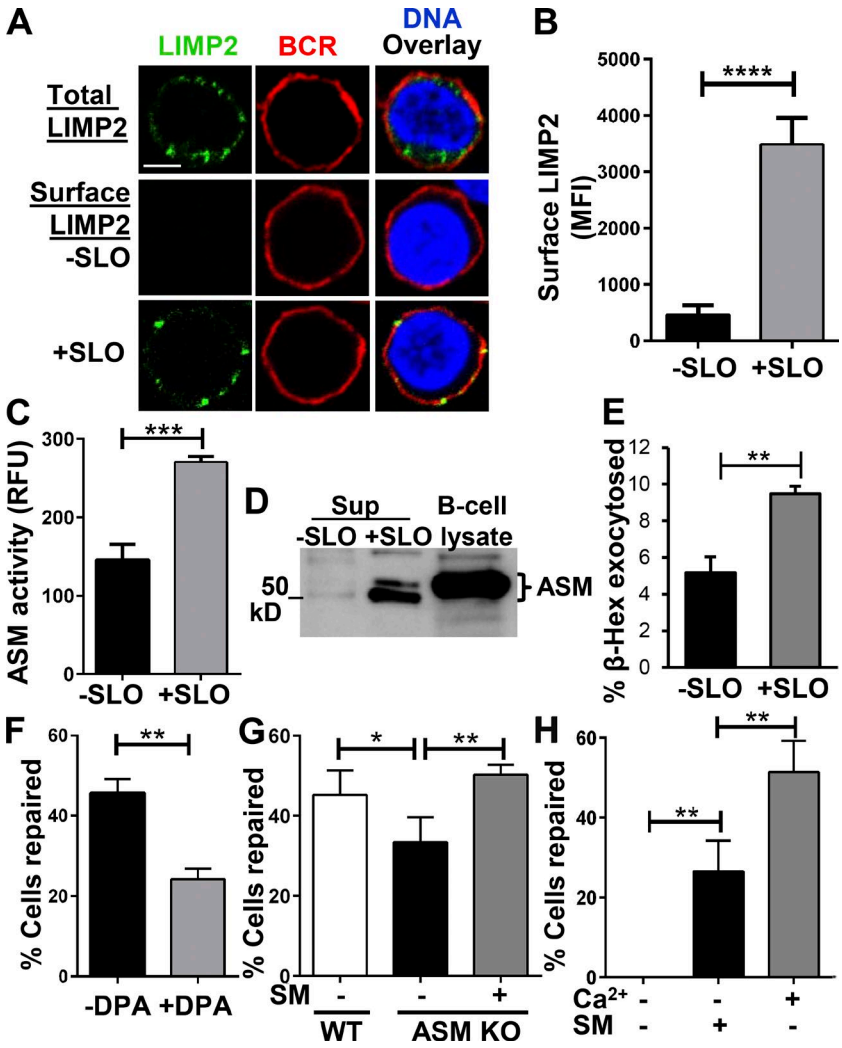

Figure 2. **PM repair in B cells depends on lysosomal exocytosis and ASM release.** (A) Immunofluorescence images of LIMP2 staining in B cells. Bar, 2.5 µm. B cells were incubated with or without SLO for 5 min at 37°C and then stained for LIMP2, BCRs, and DNA at 4°C with (total) or without permeabilization (surface). (B) The mean fluorescence intensities (MFI) of LIMP2 staining on the surface of B cells with or without SLO exposure was measured by flow cytometry. Shown is the mean (± SD) of three independent experiments. (C) The activity of ASM released from B cells into the medium. B cells were exposed to SLO for 15 s at 37°C, and ASM activity in the supernatants was detected using an Amplex red Sphingomyelinase Assay kit and expressed as relative fluorescence units (RFU). Shown is the mean (± SD) of three independent experiments. (D) ASM in whole B cell lysates or secreted after treatment with SLO for 5 min at 37°C was detected by Western blotting with anti-ASM antibodies. (E) Secretion of lysosomal β-Hex from B cells treated with SLO for 5 min at 37°C was determined in triplicate using a fluorgenic substrate and expressed as a percentage of the total activity present in whole-cell lysates. (F) Percentage of B cells repaired after exposure to SLO in the presence or absence of the ASM inhibitor DPA. B cells were preincubated with 30 µM DPA for 30 min at 37°C before and during 5-min exposure to SLO, followed by PI staining and flow cytometry. (G) Comparison of the repair efficiency of B cells from wild-type (WT) or ASM knockout (KO) mice in the presence or absence of bacterial sphingomyelinase (SM). B cells were treated with SM (50 µM) during SLO exposure, followed by PI staining and flow cytometry. (H) Comparison of the repair efficiency of wild-type B cells in the presence or absence of Ca^{2+} and SM. Shown are the mean (± SD) of three to five independent experiments. *, $P < 0.05$; **, $P < 0.005$; ***, $P < 0.001$; ****, $P < 0.0001$.

CTB endocytosis by measuring the mean fluorescence intensity (MFI) of cell-associated Alexa Fluor (AF) 488–CTB with and without addition of an AF488 quenching antibody (Fig. 3 D). We found that the MFI of quench-protected (intracellular) CTB was significantly higher in SLO-treated than in untreated B cells (Fig. 3 E). Using TEM, we determined the percentage of surface-bound biotin-CTB (marked by gold-labeled streptavidin) entering cells. We found that the number of CTB gold particles inside intracellular vesicles was increased after 1 and 5 min of SLO treatment, compared with B cells not treated with SLO (Fig. 3, F and G). Unlike what was shown in wounded fibroblasts and muscle cells (Corrotte et al., 2013), however, our TEM analysis did not observe accumulation of caveolae-like vesicles (<80-nm diameter and flask shaped) within wounded B cells (unpublished data). Collectively, these results indicate that PM wounding induces caveolae-independent and lipid raft–based endocytosis in B cells and that this endocytosis process is regulated by secretion of the lysosomal enzyme ASM.

Lipid raft–based endocytosis of CTB is important for B cell PM repair

Although B cells do not express classical caveolin, BCR signaling and endocytosis induced by antigenic ligands require a reorganization of lipid rafts (Pierce, 2002; Stoddart et al., 2002). To determine whether lipid raft endocytosis is important for B cell PM wound repair, we perturbed lipid rafts by cross-linking BCRs with antibodies, a procedure that activates receptor signaling and endocytosis similarly to bona fide antigens (Cheng et al., 1999; Liu et al., 2012). We varied the level of lipid raft perturbation by increasing the strength of BCR cross-linking. Fab fragments of anti-BCR antibody that bind but do not activate the BCR had no significant effect on the ability of B cells to repair SLO wounds (Fig. 4 A). Antibody $F(ab')_2$ fragments and biotinylated Fab plus streptavidin, both of which activate the BCR, significantly reduced the percentage of B cells that repaired SLO wounds (Fig. 4 A). Biotinylated Fab plus streptavidin, of stronger cross-linking strength than $F(ab')_2$, had a stronger inhibitory effect on PM repair than $F(ab')_2$, reducing the percentage of repaired cells >50% (Fig. 4 A). Furthermore, activation of the BCR with a gold-conjugated antibody nearly abolished SLO-induced endocytosis of CTB (Fig. 4 B). These data suggest that BCR activation inhibits PM repair in B cells, possibly by interfering with the endocytosis of lipid rafts triggered by wounding.

Repair of PM wounding by SLO inhibits formation of BCR signalosomes in lipid rafts and BCR endocytosis

Lipid rafts are critical for B cell activation by serving as a platform for both BCR signalosomes and endocytosis (Cheng et al., 1999; Sohn et al., 2008). We investigated whether the PM

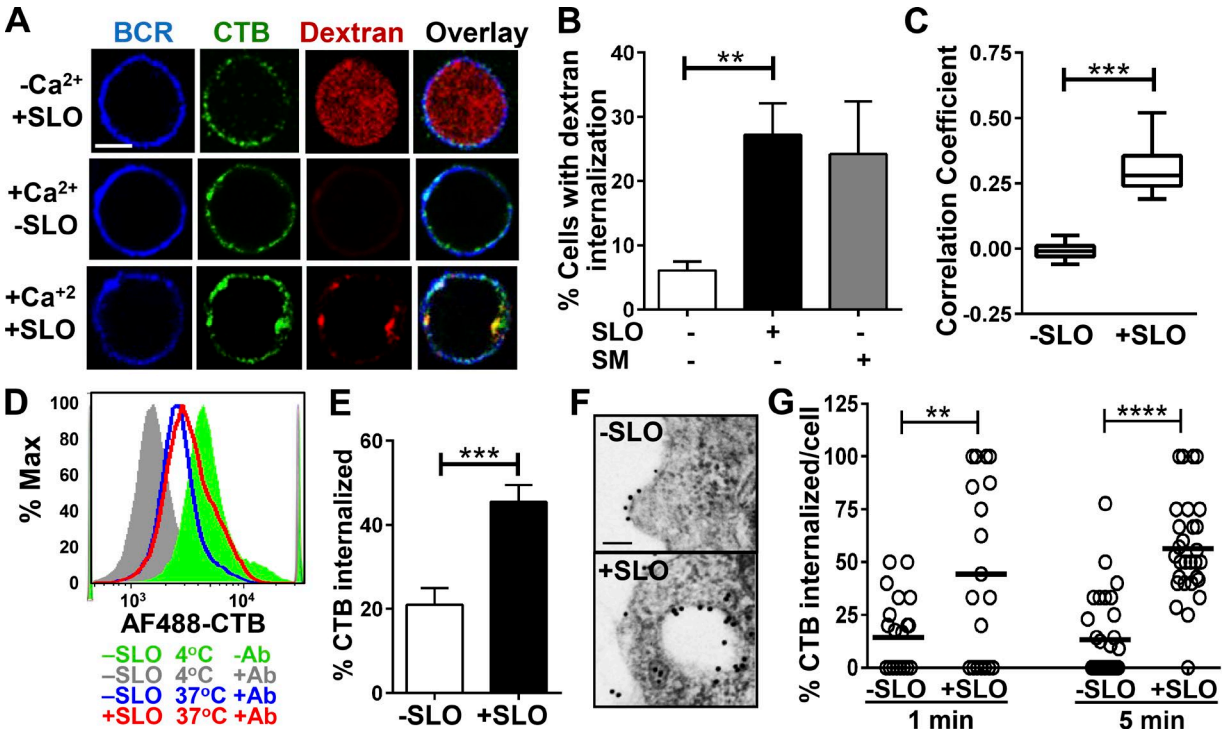

Figure 3. **PM wounding by SLO increases endocytosis.** (A) Confocal fluorescence microscopy images of Texas red–dextran and cholera toxin B subunit (CTB) in B cells. Cells were stained with Alexa Fluor (AF) 488–CTB (3 µg/ml) at 4°C and incubated with or without SLO at 37°C in the presence of dextran (2.5 mg/ml) for 3 min. Cells were then washed and stained with AF405 goat anti–mouse IgG to label surface BCR at 4°C. Bar, 2.5 µm. (B) Percentage (± SD) of B cells (treated or not with SLO or SM) showing internalized dextran, determined by visual inspection of confocal images from three independent experiments. (C) Correlation coefficients of dextran and CTB staining in the presence or absence of SLO, determined by confocal fluorescence microscopy. Shown is the mean (± SD) of three independent experiments. (D and E) Quantification of CTB endocytosis by flow cytometry. B cells were labeled with AF488-CTB (1 µg/ml) at 4°C and treated with SLO at 37°C for 3 min. The surface CTB was quenched with anti-AF488 antibodies at 4°C before and after SLO treatment. The MFI of CTB was quantified by flow cytometry. Shown are a representative histogram (D) and the percentage (± SD) of internalized CTB from three independent experiments (E). (F and G) TEM analysis of CTB endocytosis. B cells were incubated at 4°C with biotin-CTB (2 µg/ml) followed by gold-streptavidin (10 nm, 2 µg/ml), and then treated with SLO for 1 and 5 min at 37°C. Shown are representative images (F) and the mean percentage (± SD) of internalized CTB gold particles from >16 randomly selected cell profiles per condition from two independent experiments (G). Bar, 100 nm. **, P < 0.005; ****, P < 0.0001.

repair process, which also depends on lipid rafts, has any impact on the BCR signaling and antigen uptake functions. As both these functions are initiated by BCR clustering in lipid rafts, we analyzed BCR clustering and BCR-lipid raft coclustering using immunofluorescence microscopy. Surface BCRs were labeled and activated with fluorochrome-conjugated $F(ab')_2$ fragments of anti–mouse IgM+IgG antibodies, and lipid rafts by CTB. To prevent any possible effect of CTB on BCR clustering, CTB staining was performed after BCR activation and at 4°C. Similar to what we previously showed (Thyagarajan et al., 2003), BCR cross-linking induced clustering of surface BCRs to one pole of the cell, forming a polarized cap (Fig. 5 A). SLO wounding significantly reduced the percentage of B cells with BCR caps, from ∼55% to ∼35% (Fig. 5 B). Among the SLO-treated

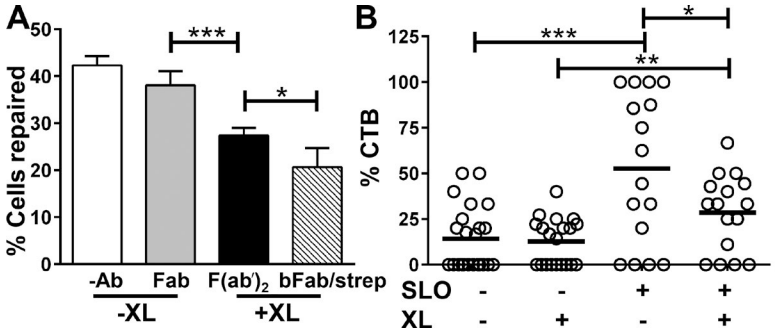

Figure 4. **BCR activation reduces the ability of B cells to repair SLO-mediated plasma membrane damage and SLO-induced CTB endocytosis.** (A) Percentage of cells repaired after SLO wounding in the presence or absence of BCR activation. B cells were incubated without (–Ab) or with Fab (10 µg/ml), $F(ab')_2$ anti–mouse IgM (10 µg/ml), or biotinylated Fab (bFab; 10 µg/ml) plus streptavidin (strep; 5 µg/ml) at 4°C and treated with SLO for 5 min at 37°C, followed by PI staining and flow cytometry. Shown is the mean (± SD) of three independent experiments. (B) The percentage of surface-labeled CTB internalized in the presence or absence of SLO and BCR cross-linking. B cells were incubated with (+XL) or without (–XL) gold anti–mouse IgM (10 µg/ml), biotin–CTB (2 µg/ml), gold-streptavidin (2 µg/ml), and SLO at 4°C and warmed up to 37°C for 1 min. Cells were then processed for TEM. The numbers of gold particles associated with and inside individual cells were counted. Shown is the mean (± SD) of >20 randomly selected cell profiles per condition from two independent experiments. *, P < 0.05; **, P < 0.01; ***, P < 0.001.

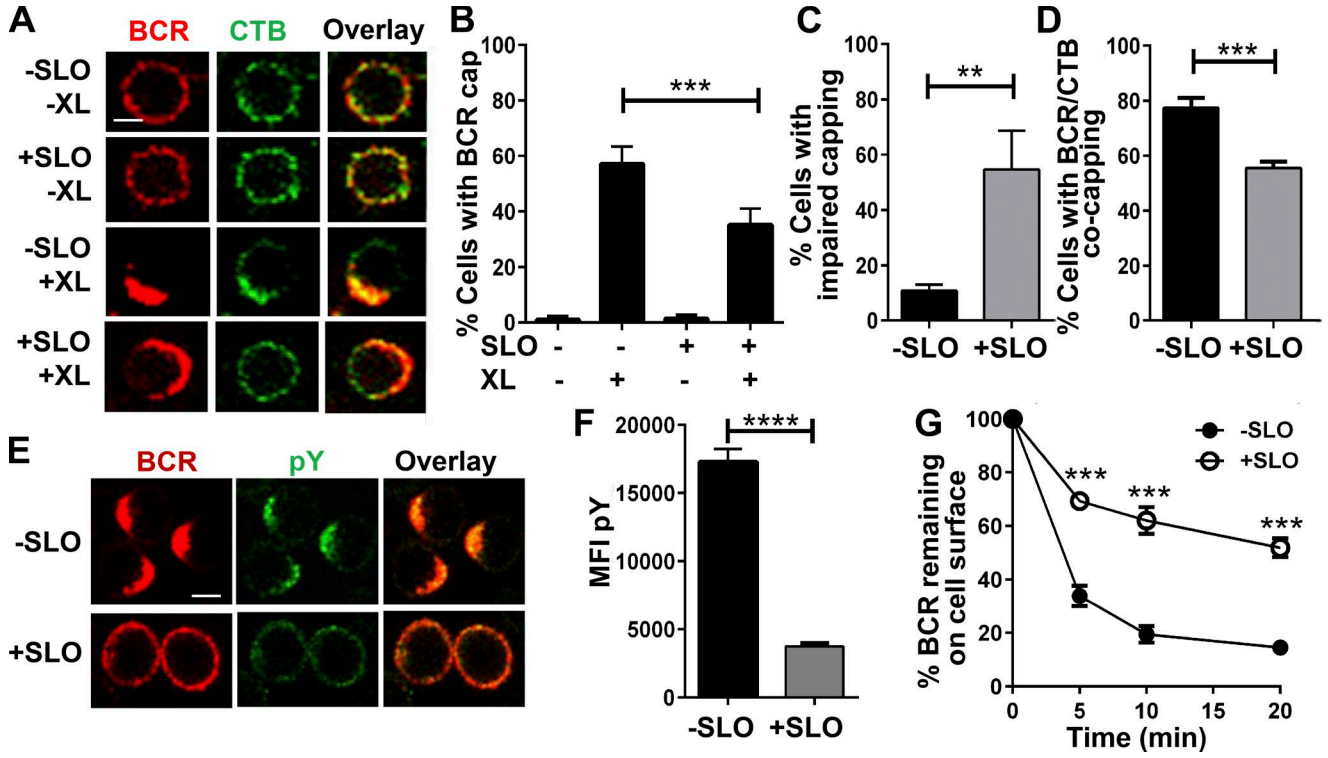

Figure 5. **SLO injury of the PM reduces BCR activation and internalization.** (A–D) BCR–CTB coclustering in the presence or absence of SLO. B cells were incubated at 4°C with Cy3-Fab (5 µg/ml; –XL) or AF546-F(ab′)$_2$ anti–mouse IgM+IgG (5 µg/ml; +XL) plus AF488-CTB (3 µg/ml) and warmed to 37°C for 5 min with or without SLO, followed by fixation and confocal microscopy. (A) Representative images. Bar, 2.5 µm. (B) Percentages (± SD) of all B cells exhibiting polarized BCR clusters (capping). (C) Percentages of B cells with polarized BCR clusters showing impaired BCR caps. (D) Percentages of B cells with polarized BCR clusters showing BCR–CTB coclustering. Data in B–D were generated by visual inspection of images from four independent experiments. (E and F) Tyrosine phosphorylation (pY) of B cells treated with or without SLO. B cells were incubated at 4°C with SLO and AF546-F(ab′)$_2$-goat anti–mouse IgM+IgG (5 µg/ml) and warmed to 37°C for 5 min, followed by fixation, permeabilization, and staining for phosphotyrosine (pY) and analysis of confocal microscopy (E) and flow cytometry (F). Shown are representative images and the mean MFI (± SD) of pY from three independent experiments. Bar, 2.5 µm. (G) Effect of SLO treatment on BCR internalization. B cells were incubated at 4°C with biotinylated F(ab′)$_2$ anti–mouse IgM+IgG (10 µg/ml), followed by 37°C incubation with or without SLO for the indicated times. Cells were then labeled with PE-streptavidin at 4°C and analyzed by flow cytometry to determine the percentage of surface-labeled BCRs remaining on the cell surface. Shown is the mean percentage (± SD) from three independent experiments. **, $P \leq 0.01$; ***, $P \leq 0.001$; ****, $P < 0.0001$.

B cells displaying polarized BCR caps, ∼50% of the caps appeared more spread out on the cell surface (impaired), compared with only 10% showing this morphology in untreated B cells (Fig. 5, A and C). In the absence of SLO, most of the B cells with BCR caps (∼75%) also showed coclustering of BCRs with CTB. SLO treatment decreased this percentage to ∼55% (Fig. 5, A and D). These results indicate that the repair of PM wounds inhibits clustering of raft-associated BCRs.

To determine whether the inhibition of BCR–CTB coclustering affects BCR signaling triggered by receptor cross-linking, we examined tyrosine phosphorylation as a measurement of signaling levels. Immunofluorescence microscopic analysis showed bright staining of antiphosphotyrosine antibody in BCR caps of untreated B cells 5 min after cross-linking. However, most of the SLO-treated cells failed to form BCR caps and exhibited much weaker and uniformly distributed phosphotyrosine staining (Fig. 5 E). Confirming the results from immunofluorescence, quantitative analysis by flow cytometry showed much lower MFI of phosphotyrosine in SLO-treated B cells when compared with untreated B cells (Fig. 5 F).

We next determined the effect of SLO-induced PM wounding on BCR endocytosis using flow cytometry. We measured the amount of reduction in surface-labeled BCR over the incubation time at 37°C, reflecting BCR endocytosis. SLO treatment reduced both the kinetics and the overall levels of BCR internalization (Fig. 5 G). At 20 min, there was more than 50% of surface-labeled BCR remaining at the surface of SLO-treated B cells, compared with ∼15% of surface-labeled BCR at the surface of untreated B cells (Fig. 5 G).

Collectively, our data demonstrate that the SLO-wounding and PM repair process inhibits both the signaling and antigen uptake functions of the BCR.

Repair of PM wounding leads to segregation of BCRs from lipid rafts

The inhibitory effect of SLO-mediated injury on the coclustering of surface BCRs with CTB suggests that the PM repair process prevents surface BCRs from interacting with lipid rafts. To investigate this hypothesis, we analyzed the colocalization between surface-labeled BCRs and CTB using live-cell imaging by confocal fluorescence microscopy. B cells that were not treated with SLO but were activated by cross-linking for 10 min showed internalization of surface labeled BCRs and colocalization of CTB with BCR-containing vesicles (Fig. 6, A and C). In contrast, there was limited colocalization between internalized BCRs and CTB in B cells that were injured by SLO (Fig. 6, A and C). We generated kymographs from time-lapse images along movement tracks of endocytosing BCRs and examined the colocalization of CTB

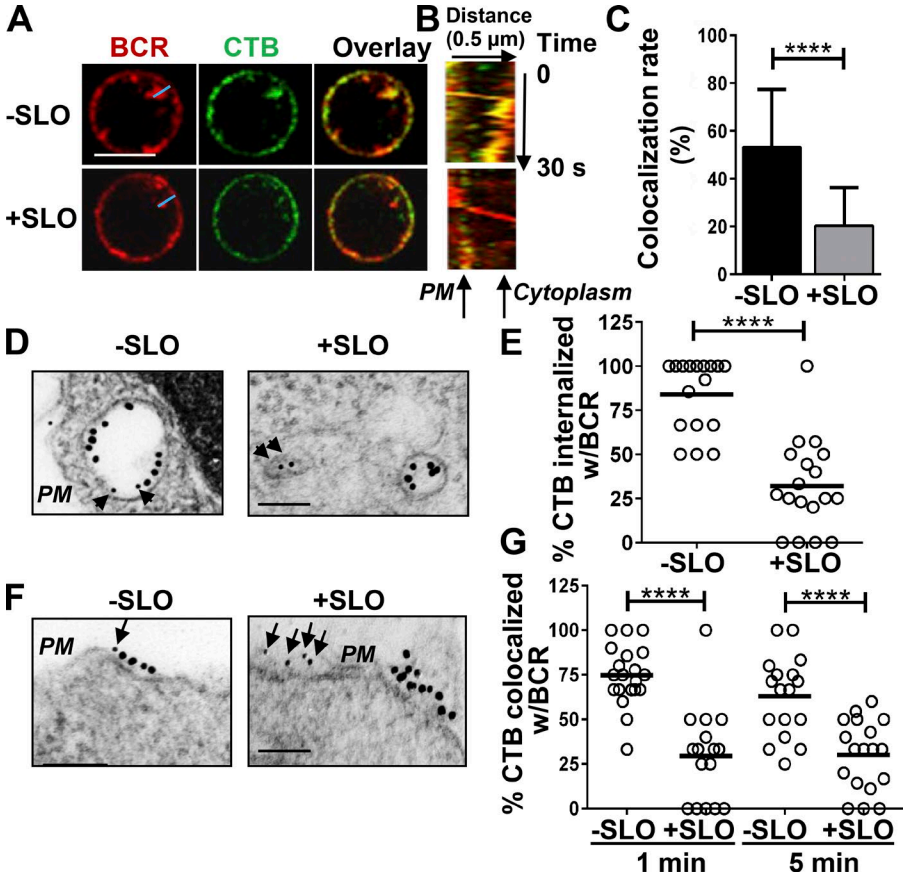

Figure 6. **PM injury by SLO segregates BCRs from CTB-labeled lipid rafts at the cell surface and during BCR internalization.** (A–C) Live-cell imaging of BCR and CTB internalization. B cells were incubated at 4°C with AF546 $F(ab')_2$ anti–mouse IgM and AF488-CTB. Time-lapse confocal images were acquired at 37°C for 10 min in the presence or absence of SLO. Shown are representative images at 10 min (A), a kymograph generated from time-lapse images along the blue line (B), and the mean colocalization rate (± SD) of BCR and CTB staining at 10 min (C), from three independent experiments. Bar, 5 µm. (D–G) TEM analysis of BCRs and CTB in B cells treated with or without SLO. B cells were incubated with gold anti–mouse IgM (18 nm, 10 µg/ml) and biotin-CTB (2 µg/ml) plus gold-streptavidin (10 nm, 2 µg/ml; arrows and arrowheads) at 4°C, and then with or without SLO at 37°C for 1 or 5 min. The percentages of CTB gold particles internalized into vesicles containing BCR gold particles at 5 min (D and E) and in the vicinity (<30 nm) of BCR gold particles at the PM (F and G) were determined in individual cell profiles. Shown are representative images (D and F) and the mean percentage (E and G) from ≥16 randomly selected cell profiles and two individual experiments. Bar, 100 nm. ****, $P < 0.0001$.

with endocytosing BCRs (yellow color) over time (Fig. 6 B). A representative kymograph from a B cell without injury showed BCR staining puncta (a BCR cluster) moving into the cells while continuously colocalizing with CTB (Fig. 6 B, top, yellow). In contrast, in B cells injured by SLO, CTB did not colocalize with BCRs when BCR clusters moved from the PM to the cytoplasm (Fig. 6 B, bottom), indicating segregation of BCRs from lipid rafts during BCR internalization.

We further confirmed this result using immunoelectron microscopy, where surface BCRs were labeled by 18-nm gold particles and CTB (Fig. 6 D, arrowheads) by 10-nm gold particles. The colocalization of BCRs with CTB was quantified in individual cells by determining the percentage of CTB gold particles in intracellular vesicles that contained BCR gold particles (Fig. 6 E). Consistent with the results of immunofluorescence microscopy, SLO treatment significantly reduced the percentage of CTB gold particles that colocalized with internalized BCRs at 5 min (Fig. 6, D and E). To determine whether CTB is segregated from BCRs at the cell surface or during endocytosis, we determined the percentage of CTB gold particles in the close vicinity of BCR gold particles on the PM using immunoelectron microscopy. We found that SLO treatment significantly reduced the percentage of CTB gold particles localized close to BCR gold particles on the B cell surface, from ∼75% and ∼60% to ∼25% at 1 and 5 min, respectively (Fig. 6, F and G). Our data demonstrate a clear segregation between BCRs and CTB-marked lipid rafts at the PM in SLO-wounded B cells. Considering that these assays were performed under conditions permissive for resealing (in the presence of Ca^{2+}), our data suggest that endocytosis-mediated removal of PM wounds interferes with the lipid raft–dependent internalization of BCRs.

BCRs and CTB are endocytosed into different types of vesicles

The segregation of BCRs from CTB during endocytosis suggests that the BCR and CTB are endocytosed into different vesicles. To investigate this hypothesis, we examined the morphology of vesicles where BCRs and CTB (5 min) were located using immunogold staining and TEM. We found irregular, tubular invaginations with no detectable clathrin coat (Fig. 7 A, a–d). Importantly, there was a significant increase in the number of the tubular invaginations in SLO-wounded B cells, compared with nonwounded B cells (Fig. 7 B). In addition to tubular invaginations, we found small, round vesicles of 120 nm or less in diameter (Fig. 7 A, e–h) and also larger vesicles (Fig. 7 A, i–l). The small vesicles often exhibited a dense clathrin-like coat (Fig. 7 A, e–g), whereas the larger vesicles showed a morphology consistent with early endosomes (Fig. 7 A, i–l). To determine in which types of membrane structures BCRs (Fig. 7 A, black arrowheads) and CTB (white arrowheads) were preferentially endocytosed, we quantified the percentage of BCR- or CTB-containing membrane structures in each category by visual inspection. We found that without SLO-induced wounds, after 5-min incubation, most of the CTB-containing membrane structures in unstimulated B cells were small vesicles (Fig. 7, A [h] and C). In the absence of SLO, BCR cross-linking did not significantly change the distribution of CTB among the different types of membrane structures. In contrast, in SLO-wounded B cells, the percentage of CTB-containing small vesicles was significantly reduced, whereas the percentage of CTB-containing uncoated tubular structures was significantly increased (Fig. 7, A and C) when compared with nonwounded cells. Conversely, BCR cross-linking reduced the percentage of CTB-containing

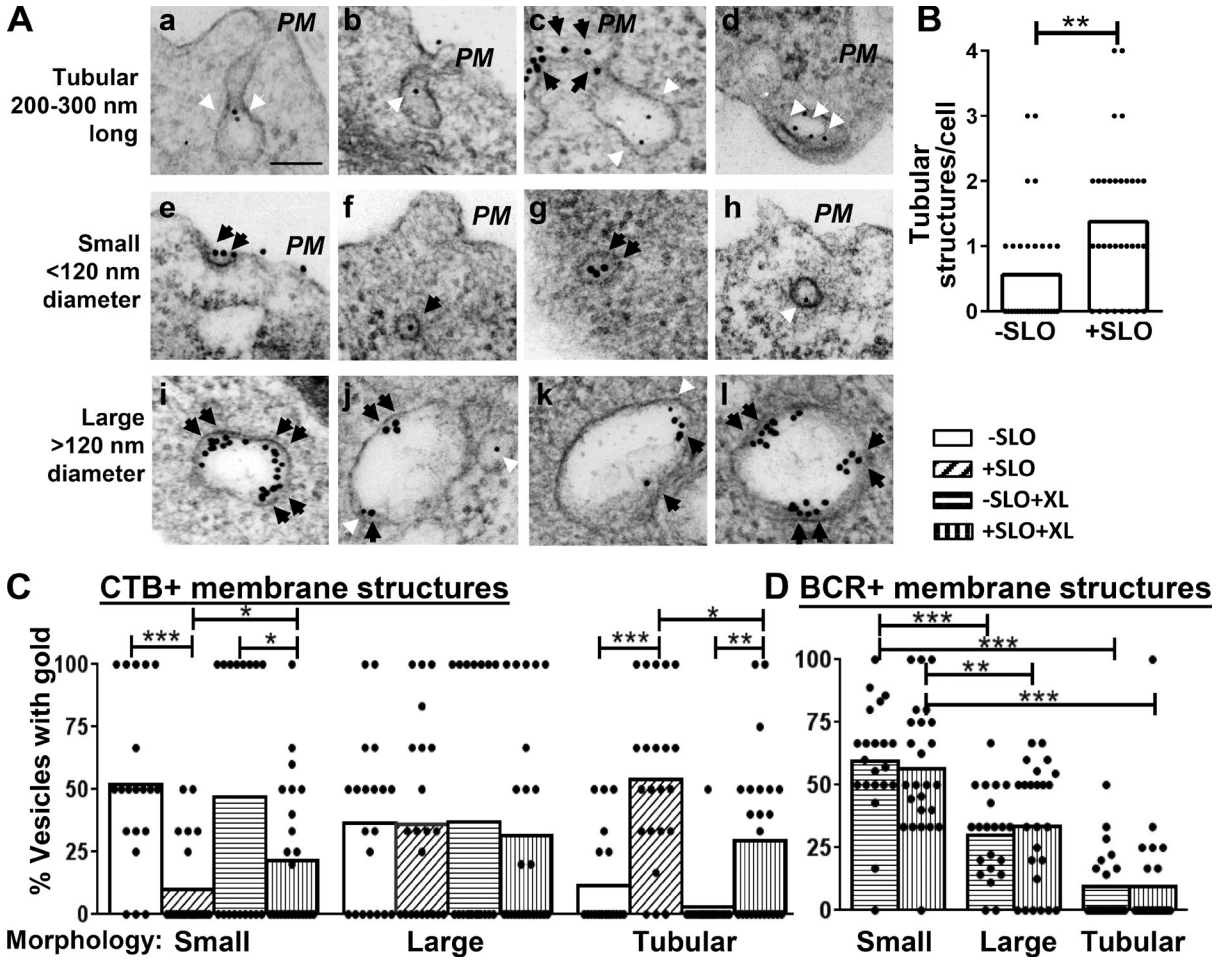

Figure 7. **Repair of PM wounds induces CTB endocytosis into uncoated tubular membrane structures.** B cells were incubated with gold anti–mouse IgM (18 nm, 10 µg/ml, black arrowheads), biotin-CTB (2 µg/ml) plus gold-streptavidin (10 nm, 2 µg/ml; white arrowheads) at 4°C and then with or without SLO at 37°C for 5 min. (A) Representative TEM images of the tubular invaginations (a–d) and small (e–h) and large vesicles (i–l). Bar, 100 nm. (B) The mean number of tubular membrane structures per cell was counted by visual inspection. (C) The mean percentages per cell of individual types of CTB-containing membrane structures among all CTB-positive vesicles. (D) The mean percentages of individual types of BCR-containing membrane structures among all BCR-positive vesicles per cell. The data were generated from ≥18 randomly selected cell profiles from two individual experiments for each condition. *, $P < 0.05$; **, $P < 0.01$; ***, $P < 0.001$.

uncoated tubular structures and increased CTB-containing small vesicles in SLO-wounded B cells (Fig. 7, A and C), suggesting a partial reversal of the effect of SLO. Similar to CTB distribution in nonwounded B cells, BCRs were preferentially localized in small coated vesicles after 5-min incubation in unwounded B cells, whereas BCR gold particles were mostly excluded from uncoated tubular structures (Fig. 7, A [c] and D). In contrast to the effects of SLO-caused wounds on CTB redistribution into uncoated tubular structures, SLO treatment did not significantly change the preferential location of endocytosing BCRs in small coated vesicles (Fig. 7 D). These results suggest that PM wounding and repair induce endocytosis of lipid raft–bound CTB through uncoated tubular invaginations, which exclude BCRs.

Discussion

This study demonstrates that primary mouse B lymphocytes rapidly repair PM wounds caused by the bacterial pore-forming toxin SLO, in a Ca^{2+}-dependent manner. The B cell repair process involves lysosomal exocytosis triggered by Ca^{2+} influx through the wounds and a clathrin-independent, lipid raft–dependent form of endocytosis that can be induced by the lysosomal enzyme ASM. Importantly, ligand engagement of the BCR, which induces BCR clustering, signaling, and internalization via lipid rafts (Cheng et al., 1999; Pierce, 2002), interferes with PM repair. Conversely, PM repair suppresses the signaling and antigen uptake functions of the BCR. The mutual suppression between BCR activation and PM repair observed in this study uncovers a critical role of lipid rafts in regulating B cell PM repair.

Several lines of evidence indicate that the mutual inhibition observed between PM wound repair and BCR signaling/endocytosis is not a consequence of generalized, nonspecific effects on B cell physiology. First, the timing of the two events is different. PM repair is completed within 30 s of wounding (Steinhardt et al., 1994; Andrews et al., 2014), which is essential for saving cells from catastrophic death as a result of massive Ca^{2+} influx. In contrast, BCR signaling and internalization occurs on a time scale of minutes, requiring the formation and growth of BCR clusters, followed by clathrin-mediated endocytosis (Tolar et al., 2009; Song et al., 2013). Because PM wounds are already repaired when BCR signaling and endocytosis are initiated, downstream effects of BCR signaling and endocytosis on PM repair should be negligible. Rather, our data suggest that

engagement of lipid rafts as an early step of the BCR clustering process reduces the availability of membrane microdomains with the properties required for ASM-dependent endocytosis of wounded membrane. Second, to minimize any potential indirect impact of PM wounding on the early steps of BCR engagement and signaling, we excluded from our analysis cells that were not able to completely reseal their PM within the assay period. Finally, segregation of the BCR and CTB in wounded cells is detected on the PM before endocytosis, supporting the conclusion that the mutual inhibition is mediated via an early event driven by membrane reorganization.

Our results show that B cells repair PM wounds using mechanisms that have several elements in common with those reported for muscle, fibroblasts, and epithelial cells: Ca^{2+}-induced lysosomal exocytosis followed by ASM-induced endocytosis (Idone et al., 2008; Tam et al., 2010; Corrotte et al., 2012, 2013). ASM inhibition or depletion reduced the ability of B cells to repair their PM, and the repair ability of ASM-deficient B cells was restored by extracellular SM. Exogenously added SM was also sufficient to promote PM repair of B cells in the absence of Ca^{2+}, strongly suggesting that the B lymphocyte resealing mechanism is driven by generation of ceramide on the outer leaflet of the PM, as proposed for other cell types (Corrotte et al., 2013). However, B cells from ASM knockout mice showed a smaller reduction in their repair capability when compared with B cells treated with ASM inhibitor, or in Ca^{2+}-free media. This result suggests that other factors, perhaps also released from lysosomes by Ca^{2+}-triggered exocytosis, are involved in B cell PM repair. Alternatively, ASM gene deletion in mice may enhance the expression of factors that compensate for the loss of ASM function.

CTB, used in our study as a marker for lipid rafts, can be endocytosed via multiple mechanisms including caveolin-dependent and clathrin-dependent and independent pathways, depending on the expression levels of caveolin and clathrin (Torgersen et al., 2001; Singh et al., 2003; Chinnapen et al., 2007; Ewers and Helenius, 2011). However, the mechanisms by which lipid rafts and CTB are endocytosed in B cells remain poorly understood. Although BCR endocytosis is mainly mediated by a clathrin-dependent pathway, it also requires lipid rafts (Brodsky et al., 1989; Guagliardi et al., 1990; Stoddart et al., 2002). Lipid rafts are thought to provide the platform where clathrin is phosphorylated and gains access to the BCR to be endocytosed (Pierce, 2002; Stoddart et al., 2002). In this study, we found that CTB and BCRs colocalize during endocytosis in intact cells. Upon PM wounding, CTB is segregated from BCRs on the PM and enriched in noncoated tubular invaginations. Our results suggest that CTB switches from a clathrin- and raft-dependent to a clathrin-independent and raft-dependent endocytic pathway in response to PM wounding. Therefore, in B cells, CTB appears to follow the bulk distribution of lipid raft domains in these cells.

Our studies revealed a unique characteristic of the PM repair mechanism in B cells: PM wounding induces a form of endocytosis that is lipid raft dependent but independent of caveolae. Caveolin, a protein required for caveolae formation, inserts its lipidated hydrophobic domain into the inner leaflet of membrane microdomains rich in cholesterol and sphingolipids, which are defining characteristics of lipid rafts (Galbiati et al., 2001; Nabi and Le, 2003). Caveolae are also known to mediate endocytosis of proteins associated with lipid rafts (Nabi and Le, 2003). B lymphocytes, however, do not express detectable amounts of the three known isoforms of caveolin and consequently do not appear to form caveolae (Fra et al., 1994). Corrotte et al. reported that the repair of both SLO and mechanical wounds in muscle fibers and epithelial cells requires ASM and an endocytic process involving caveolae (Corrotte et al., 2013). Consistent with the lack of caveolae in B cells, in this study, we did not observe an intracellular accumulation of vesicles resembling classical caveolae (~80-nm diameter with flask- or omega-shaped PM invaginations; Parton and Simons, 2007) immediately after PM wounding, as reported by Corrotte et al. (2013) for other cell types. Interestingly, our results show a clear link between the ability of B cells to repair PM wounds and the rapid formation of tubular membrane invaginations with properties of lipid rafts. Thus, our results suggest that a common requirement for the process of PM repair might be the mobilization of lipid raft domains for endocytosis, with the specific form of endocytosis varying depending on the expression of specific factors such as caveolin.

These observations raise the question of how endocytosis of lipid rafts triggered by PM wounding is induced without the participation of clathrin or caveolin. In wounded muscle fibers, epithelial cells and fibroblasts, caveolae-mediated endocytosis of wounded PM is induced by exocytosed ASM (Tam et al., 2010; Corrotte et al., 2013). ASM converts sphingomyelin into ceramide, creating ceramide-enriched membrane microdomains that can trigger invagination of lipid bilayers (Holopainen et al., 2000; Trajkovic et al., 2008). Here, we show that wound-induced endocytosis in B cells also depends on extracellular ASM. In the absence of caveolin, B cell wounding induces formation of uncoated tubular PM invaginations that mediate endocytosis of lipid raft–binding CTB. Although the identity of this tubular endocytic pathway remains to be defined, CTB has been shown to be endocytosed in tubular structures in the absence of caveolin (Kirkham et al., 2005). Furthermore, a characteristic of the clathrin- and caveolin-independent endocytic pathway is to internalize surface molecules through tubular invaginations (Kirkham and Parton, 2005; Mayor and Pagano, 2007). Thus, our results suggest that ceramide generation by ASM released by lysosomal exocytosis induces lipid raft endocytosis via a tubular, caveolin-, and clathrin-independent pathway in B cells. Further investigations should clarify if this pathway shares properties with clathrin- and caveolin-independent endocytic pathways described in other cell types.

We were unable to examine the repair of PM wounds provoked by mechanical forces in B cells because of their high vulnerability to shearing force. Although mechanical wounding causes a form of membrane damage that is presumed to be different from SLO, which forms small pores after binding to cholesterol, the repair of both types of membrane wounds is mediated via rapid ASM-induced caveolae-mediated endocytosis (Corrotte et al., 2013). This suggests that in B cells, the repair of SLO pores and mechanical wounds may also involve local generation of ceramide from sphingomyelin and the rapid endocytosis of lipid raft portions of the PM, a process that is functionally equivalent to the caveolar endocytosis described in cell types that express caveolin.

Segregation of BCRs from lipid rafts was shown to impair the BCR phosphorylation by Src kinases required for initiating signaling (Cheng et al., 1999) and the interaction of clathrin with BCR aggregates (Stoddart et al., 2002). Thus, PM wounding and repair is expected to have an inhibitory effect in B cell function. Although B cell membrane damage has not yet been studied in vivo, these cells are frequently in an envi-

ronment that is likely to cause PM wounding. In addition to encountering pore-forming toxins of pathogens directly, B cells circulate through narrow blood vessels at high velocity, undergo chemotaxis from blood vessels to infection sites, and migrate through lymphatic organs, an extremely crowded environment. Furthermore, when B cells present antigen to T cells or other B cells, fragments of their PM can be extracted with the antigen by antigen-acquiring cells (Quah et al., 2008; Hwang and Ki, 2011; Natkanski et al., 2013). We show here that B cells possess a rapid, Ca^{2+}-dependent PM repair mechanism that protects them from wounding-induced death. The inhibitory effect of the PM repair process on BCR activation, which we uncovered here, likely suppresses BCR-mediated activation of B cells that are injured by presenting antigen or migrating through narrow spaces. Although the physiological significance of this phenomenon remains to be defined, reductions in BCR signaling and antigen uptake may reshape B cell functional status. First, the inhibition of antigen uptake and processing enables B cells to become better antigen-presenting cells to other B cells. Second, the inhibition of BCR signaling may facilitate the progress of B cells that present antigen to T cells toward BCR-independent and T cell–dependent activation and differentiation. Marginal zone B cells belong to a subset of mature B cells that are capable of shuttling antigens from the marginal zone to secluded regions of B cell follicles in the secondary lymph organs (Batista and Harwood, 2009). The inhibitory effects of B cell PM damage and repair, possibly provoked by migration and antigen presentation, may impair the activation and antigen internalization activities of marginal zone B cells, enhancing their antigen shuttling function. Although this hypothesis remains to be tested, our results provide a potential mechanistic explanation for the unique capability of marginal zone B cells to shuttle antigen.

Materials and methods

Mice and B cell isolation

Splenic B cells were isolated from wild-type (C57BL/6; Jackson ImmunoResearch Laboratories) and ASM knockout mice in C57BL/6 background (provided by E. Schuchman, Mount Sinai School of Medicine, New York, NY, and S. Muro, University of Maryland, Baltimore, MD). The *ASM* gene in ASM knockout mice was disrupted by an insertion of the PGK*neo* expression cassette into the exon 2 (Horinouchi et al., 1995). Mononuclear cells were enriched by Ficoll density-gradient centrifugation (Sigma-Aldrich). T cells were removed by rat anti-Thy1.2 mAb (BD Biosciences) and guinea pig complement (Rockland Immunochemicals) and monocytes and dendritic cells by panning. All procedures involving mice were approved by the Institutional Animal Care and Usage Committee of the University of Maryland.

PM repair assays

Freshly isolated B cells were incubated with SLO in either Ca^{2+}-containing ($+Ca^{2+}$) or Ca^{2+}-free DMEM ($-Ca^{2+}$) for 5 min at 4°C to allow binding. Cells were then warmed to 37°C for 5 min, immediately transferred to 4°C, and stained with the membrane impermeant dye PI. Cells were analyzed using a BD FACS Canto II flow cytometer and FlowJo software (Tree Star). The percentage of cells repaired in the presence of Ca^{2+} ($+Ca^{2+}$) was determined by [%PI positive ($-Ca^{2+}$) − %PI positive ($+Ca^{2+}$)] × 100/%PI positive ($-Ca^{2+}$).

To determine the effect of SM on PM repair, SM from *Bacillus cereus* (50 µM; Sigma-Aldrich) was included in the medium during the 37°C incubation.

To analyze the effect of BCR cross-linking on the efficacy of PM repair, surface BCR were bound with Fab fragments of goat anti–mouse IgM (10 µg/ml) that does not cross-link BCRs (−XL), $F(ab')_2$ fragment of goat anti–mouse IgM (10 µg/ml; Jackson ImmunoResearch Laboratories) that cross-links BCRs (+XL) for 20 min at 4°C, or biotinylated Fab goat anti–mouse IgM (10 µg/ml; Jackson ImmunoResearch Laboratories) for 20 min at 4°C plus streptavidin (5 µg/ml; Jackson ImmunoResearch Laboratories) at 4°C for 10 min for extensive cross-linking of BCRs. After washing off unbound antibodies/streptavidin, the cells were then treated with SLO (200 ng/ml) and analyzed by flow cytometry as described above.

Analyses of lysosomal exocytosis

B cells were incubated without or with SLO (200 ng/ml) for 5 min at 4°C and then 37°C for 5 min. To stain LIMP2 at the cell surface, cells were transferred to 4°C, incubated with rabbit anti-LIMP2 antibody (5 µg/ml; Sigma-Aldrich), followed by AF488 goat anti–rabbit IgG (5 µg/ml; Invitrogen) as secondary antibody and Cy3-Fab-goat anti–mouse IgM+IgG (5 µg/ml; Jackson ImmunoResearch Laboratories) for marking BCRs at 4°C without permeabilization. Cells were then washed to remove all unbound antibodies and fixed with 4% paraformaldehyde. For intracellular LIMP2 staining, B cells were fixed with 4% paraformaldehyde after surface staining of BCRs at 4°C, permeabilized with 0.05% saponin, and stained with rabbit anti-LIMP2 antibody, followed by AF488-goat anti–rabbit IgG and postfixation. Cells were analyzed by flow cytometry (BD FACS Canto II) and confocal fluorescence microscopy (100× oil objective 1.4 NA, LSM 710; Carl Zeiss).

To quantify lysosome exocytosis, the percentage of β-hex secreted was determined by its enzymatic activity, using 4-methylumbelliferyl-*N*-acetyl-β-D-glucosaminide dehydrate (Sigma-Aldrich) as a substrate (Rodríguez et al., 1997). After primary B cells were treated with or without 200 ng/ml SLO for 5 min at 37°C, the supernatants were collected. The enzymatic activity of β-hex in the supernatant was determined as the portion of secreted. The total cell-associated β-hex activity was determined using the lysate of SLO-untreated B cells. The percentage of β-hex secretion was calculated based on the enzymatic activity ratio of β-hex in the supernatant to that in the cell lysate.

ASM secretion and inhibition

The secretion of ASM was analyzed by measuring the enzymatic activity of ASM in supernatants. Cells were treated with SLO (200 ng/ml) for 5 min at 4°C, warmed to 37°C for 15 s, and immediately cooled on ice. The supernatants were collected by centrifugation, and protease inhibitors added. The enzymatic activity of ASM was determined using an Amplex red sphingomyelinase assay kit (Molecular Probes), based on manufacturer-provided protocols. Supernatants were also concentrated using centrifugal filtration (Millipore) and analyzed by Western blotting, using rabbit anti-ASM antibody (Abcam).

To inhibit ASM, B cells were preincubated with 30 µM DPA (Sigma-Aldrich) for 30 min at 37°C. Cells were then treated with SLO in the presence of DPA and stained with PI as described in the PM repair assays section.

Dextran and CTB internalization

For immunofluorescence microscopic analysis, B cells were stained with AF488-CTB (3 µg/ml; Invitrogen) for 10 min at 4°C, washed, and then incubated with SLO (200 ng/ml) for 5 min at 4°C. After addition of 10 kD lysine fixable Texas red–dextran (2.5 mg/ml; Invitrogen) to the media, the cells were warmed to 37°C for 3 min, washed to remove dextran that was not associated with cells, and then stained with AF405-goat anti–mouse IgG (Invitrogen) at 4°C to mark surface BCRs. Cells were fixed and imaged by confocal fluorescence microscopy (100× oil

objective 1.4 NA; LSM 710). For SM treatment, cells were incubated with 50 µM SM (Sigma-Aldrich) during the 37°C incubation. Correlation coefficients between dextran and CTB were determined using ZEN imaging software (Carl Zeiss).

For flow cytometry analysis of CTB internalization, B cells were stained with AF488-CTB (1 µg/ml; Invitrogen) for 10 min at 4°C and washed. Surface-bound AF488-CTB were quenched with a rabbit anti-AF488 antibody (Invitrogen) at 4°C either before or after incubation with SLO (200 ng/ml) 3 min at 37°C. The MFI of AF488-CTB before and after quench were determined using flow cytometry (BD FACS Canto II). The total surface labeled CTB was determined as the difference of the CTB MFI before and after quench without SLO treatment at 37°C. The internalized CTB was quantified as the CTB MFI of SLO-treated cells after quench. The percentage of CTB internalization was calculated by the ratio of the internalized CTB to the total surface-labeled CTB multiplied by 100.

BCR capping and activation

B cells were labeled and/or activated with Cy3-Fab goat anti–mouse IgM+IgG (5 µg/ml; Jackson ImmunoResearch Laboratories) or AF546-$F(ab')_2$ goat anti–mouse IgM+IgG (5 µg/ml; Invitrogen) at 4°C for 20 min, followed by AF488-CTB (3 µg/ml; Invitrogen) for 10 min. Cells were washed to remove unbound antibody and CTB, and then incubated with SLO (200 ng/ml) for 5 min at 4°C, warmed to 37°C for 5 min, and fixed with 4% paraformaldehyde. Cells were imaged using a confocal microscope (63× oil objective 1.4 NA; LSM 710). For each condition, >80 cells were analyzed for each of four independent experiments.

For phosphotyrosine staining, B cells were permeabilized with 0.05% saponin and incubated with mouse IgG_{2b} antiphosphotyrosine mAb 4G10 (Millipore), followed by AF488-goat anti–mouse IgG_{2b} secondary antibody (Invitrogen). Cells were analyzed by confocal microscopy (63× oil objective 1.4 NA; LSM 710) and flow cytometry (BD FACS Canto II).

Flow cytometry analysis of BCR endocytosis

The surface BCRs were labeled at 4°C with biotinylated $F(ab')_2$ goat anti–mouse IgM+IgG (10 µg/ml; Jackson ImmunoResearch Laboratories) for 30 min. The cells were washed to remove unbound antibody and then incubated with or without SLO (200 ng/ml) at 4°C for 5 min, warmed to 37°C, and fixed at indicated times. The biotinylated $F(ab')_2$-goat anti–mouse IgM+IgG that remained at the cell surface were then detected with PE–streptavidin (3 µg/ml; BD Bioscience) and quantified using flow cytometry (BD FACS Canto II) and FlowJo software.

Live-cell imaging of BCR–CTB internalization

The surface BCRs were labeled and activated with AF546-$F(ab')_2$ goat anti–mouse IgM (5 µg/ml; Invitrogen) and lipid rafts by AF488-CTB (3 µg/ml; Invitrogen) at 4°C. After 5-min incubation with SLO (200 ng/ml) at 4°C, time-lapse images were acquired at 37°C using an SP5 confocal fluorescence microscope (63× oil objective 1.4 NA; Leica). Kymographs were constructed using Andor IQ (Andor Technology) to track the internalization of BCR and CTB over time. The colocalization rate (percentage of pixel overlap of two colors) of internalized BCRs with CTB at 10 min was determined using Leica LAS AF Lite imaging software. For each condition, more than eight cells were analyzed for each of three independent experiments.

Immunoelectron microscopy analysis of BCR and CTB distribution

The surface BCRs were labeled with 18-nm gold-conjugated goat anti–mouse IgM (10 µg/ml; Jackson ImmunoResearch Laboratories) and lipid rafts by biotinylated CTB (2 µg/ml; Invitrogen) followed by 10-nm gold-conjugated streptavidin (2 µg/ml; Sigma-Aldrich) at 4°C. Cells were then incubated with SLO (200 ng/ml) for 5 min at 4°C, warmed to 37°C for 1 and 5 min, and fixed with 2% glutaraldehyde. The cells were post-fixed by 2% osmium tetroxide, embedded in Spurr's replacement embedding medium (Electron Microscopy Sciences), and imaged by transmission electron microscopy (EM 10CA; Carl Zeiss). For each condition, ≥18 individual cells were analyzed for each of two independent experiments.

Statistical analysis

Statistical analysis was performed by the two-tailed *t* test using Prism software (GraphPad Software).

Acknowledgments

We thank E.H. Schuchman and S. Muro for providing ASM mice, A. Beaven (Cell Biology and Molecular Genetics [CBMG] Imaging Core, University of Maryland) and Ken Class (CBMG Flow Cytometry Core, University of Maryland) for assistance with confocal microscopy and flow cytometry, the Maryland Stem Cell Research Fund for funding, and the members of the Song laboratory for helpful discussions.

Work in the Andrews Laboratory was supported by the National Institutes of Health grant R01 GM064625.

The authors declare no competing financial interests.

Submitted: 7 May 2015
Accepted: 18 November 2015

References

Andrews, N.W., P.E. Almeida, and M. Corrotte. 2014. Damage control: cellular mechanisms of plasma membrane repair. *Trends Cell Biol.* 24:734–742. http://dx.doi.org/10.1016/j.tcb.2014.07.008

Bansal, D., K. Miyake, S.S. Vogel, S. Groh, C.C. Chen, R. Williamson, P.L. McNeil, and K.P. Campbell. 2003. Defective membrane repair in dysferlin-deficient muscular dystrophy. *Nature.* 423:168–172. http://dx.doi.org/10.1038/nature01573

Batista, F.D., and N.E. Harwood. 2009. The who, how and where of antigen presentation to B cells. *Nat. Rev. Immunol.* 9:15–27. http://dx.doi.org/10.1038/nri2454

Bléry, M., L. Tze, L.A. Miosge, J.E. Jun, and C.C. Goodnow. 2006. Essential role of membrane cholesterol in accelerated BCR internalization and uncoupling from NF-kappa B in B cell clonal anergy. *J. Exp. Med.* 203:1773–1783. http://dx.doi.org/10.1084/jem.20060552

Brandes, M., D.F. Legler, B. Spoerri, P. Schaerli, and B. Moser. 2000. Activation-dependent modulation of B lymphocyte migration to chemokines. *Int. Immunol.* 12:1285–1292. http://dx.doi.org/10.1093/intimm/12.9.1285

Brodsky, F.M., B. Koppelman, J.S. Blum, M.S. Marks, P. Cresswell, and L. Guagliardi. 1989. Intracellular colocalization of molecules involved in antigen processing and presentation by B cells. *Cold Spring Harb. Symp. Quant. Biol.* 54:319–331. http://dx.doi.org/10.1101/SQB.1989.054.01.040

Chen, W.T. 1981. Mechanism of retraction of the trailing edge during fibroblast movement. *J. Cell Biol.* 90:187–200. http://dx.doi.org/10.1083/jcb.90.1.187

Cheng, P.C., M.L. Dykstra, R.N. Mitchell, and S.K. Pierce. 1999. A role for lipid rafts in B cell antigen receptor signaling and antigen targeting. *J. Exp. Med.* 190:1549–1560. http://dx.doi.org/10.1084/jem.190.11.1549

Cheng, P.C., B.K. Brown, W. Song, and S.K. Pierce. 2001. Translocation of the B cell antigen receptor into lipid rafts reveals a novel step in signaling. *J. Immunol.* 166:3693–3701. http://dx.doi.org/10.4049/jimmunol.166.6.3693

Chinnapen, D.J., H. Chinnapen, D. Saslowsky, and W.I. Lencer. 2007. Rafting with cholera toxin: endocytosis and trafficking from plasma membrane to ER. *FEMS Microbiol. Lett.* 266:129–137. http://dx.doi.org/10.1111/j.1574-6968.2006.00545.x

Clarke, M.S., R.W. Caldwell, H. Chiao, K. Miyake, and P.L. McNeil. 1995. Contraction-induced cell wounding and release of fibroblast growth factor in heart. *Circ. Res.* 76:927–934. http://dx.doi.org/10.1161/01.RES.76.6.927

Corrotte, M., M.C. Fernandes, C. Tam, and N.W. Andrews. 2012. Toxin pores endocytosed during plasma membrane repair traffic into the lumen of MVBs for degradation. *Traffic.* 13:483–494. http://dx.doi.org/10.1111/j.1600-0854.2011.01323.x

Corrotte, M., P.E. Almeida, C. Tam, T. Castro-Gomes, M.C. Fernandes, B.A. Millis, M. Cortez, H. Miller, W. Song, T.K. Maugel, and N.W. Andrews. 2013. Caveolae internalization repairs wounded cells and muscle fibers. *eLife.* 2:e00926. http://dx.doi.org/10.7554/eLife.00926

Dal Porto, J.M., S.B. Gauld, K.T. Merrell, D. Mills, A.E. Pugh-Bernard, and J. Cambier. 2004. B cell antigen receptor signaling 101. *Mol. Immunol.* 41:599–613. http://dx.doi.org/10.1016/j.molimm.2004.04.008

Ewers, H., and A. Helenius. 2011. Lipid-mediated endocytosis. *Cold Spring Harb. Perspect. Biol.* 3:a004721. http://dx.doi.org/10.1101/cshperspect.a004721

Fra, A.M., E. Williamson, K. Simons, and R.G. Parton. 1994. Detergent-insoluble glycolipid microdomains in lymphocytes in the absence of caveolae. *J. Biol. Chem.* 269:30745–30748.

Galbiati, F., B. Razani, and M.P. Lisanti. 2001. Emerging themes in lipid rafts and caveolae. *Cell.* 106:403–411. http://dx.doi.org/10.1016/S0092-8674(01)00472-X

Gazzerro, E., F. Sotgia, C. Bruno, M.P. Lisanti, and C. Minetti. 2010. Caveolinopathies: from the biology of caveolin-3 to human diseases. Eur. J. Hum. Genet. 18:137–145.

Geeraerts, M.D., M.F. Ronveaux-Dupal, J.J. Lemasters, and B. Herman. 1991. Cytosolic free Ca2+ and proteolysis in lethal oxidative injury in endothelial cells. *Am. J. Physiol.* 261:C889–C896.

Grassmé, H., V. Jendrossek, J. Bock, A. Riehle, and E. Gulbins. 2002. Ceramide-rich membrane rafts mediate CD40 clustering. *J. Immunol.* 168:298–307. http://dx.doi.org/10.4049/jimmunol.168.1.298

Guagliardi, L.E., B. Koppelman, J.S. Blum, M.S. Marks, P. Cresswell, and F.M. Brodsky. 1990. Co-localization of molecules involved in antigen processing and presentation in an early endocytic compartment. *Nature.* 343:133–139. http://dx.doi.org/10.1038/343133a0

Hagiwara, Y., T. Sasaoka, K. Araishi, M. Imamura, H. Yorifuji, I. Nonaka, E. Ozawa, and T. Kikuchi. 2000. Caveolin-3 deficiency causes muscle degeneration in mice. *Hum. Mol. Genet.* 9:3047–3054. http://dx.doi.org/10.1093/hmg/9.20.3047

Hat, B., B. Kazmierczak, and T. Lipniacki. 2011. B cell activation triggered by the formation of the small receptor cluster: a computational study. *PLOS Comput. Biol.* 7:e1002197. http://dx.doi.org/10.1371/journal.pcbi.1002197

Hnasko, R., and M.P. Lisanti. 2003. The biology of caveolae: lessons from caveolin knockout mice and implications for human disease. *Mol. Interv.* 3:445–464. http://dx.doi.org/10.1124/mi.3.8.445

Holopainen, J.M., M.I. Angelova, and P.K. Kinnunen. 2000. Vectorial budding of vesicles by asymmetrical enzymatic formation of ceramide in giant liposomes. *Biophys. J.* 78:830–838. http://dx.doi.org/10.1016/S0006-3495(00)76640-9

Horinouchi, K., S. Erlich, D.P. Perl, K. Ferlinz, C.L. Bisgaier, K. Sandhoff, R.J. Desnick, C.L. Stewart, and E.H. Schuchman. 1995. Acid sphingomyelinase deficient mice: a model of types A and B Niemann-Pick disease. *Nat. Genet.* 10:288–293. http://dx.doi.org/10.1038/ng0795-288

Hwang, I., and D. Ki. 2011. Receptor-mediated T cell absorption of antigen presenting cell-derived molecules. *Front. Biosci. (Landmark Ed.).* 16:411–421. http://dx.doi.org/10.2741/3695

Idone, V., C. Tam, J.W. Goss, D. Toomre, M. Pypaert, and N.W. Andrews. 2008. Repair of injured plasma membrane by rapid Ca2+-dependent endocytosis. *J. Cell Biol.* 180:905–914. http://dx.doi.org/10.1083/jcb.200708010

Jaiswal, J.K., N.W. Andrews, and S.M. Simon. 2002. Membrane proximal lysosomes are the major vesicles responsible for calcium-dependent exocytosis in nonsecretory cells. *J. Cell Biol.* 159:625–635. http://dx.doi.org/10.1083/jcb.200208154

Kirkham, M., and R.G. Parton. 2005. Clathrin-independent endocytosis: new insights into caveolae and non-caveolar lipid raft carriers. *Biochim. Biophys. Acta.* 1745:273–286. http://dx.doi.org/10.1016/j.bbamcr.2005.06.002

Kirkham, M., A. Fujita, R. Chadda, S.J. Nixon, T.V. Kurzchalia, D.K. Sharma, R.E. Pagano, J.F. Hancock, S. Mayor, and R.G. Parton. 2005. Ultrastructural identification of uncoated caveolin-independent early endocytic vehicles. *J. Cell Biol.* 168:465–476. http://dx.doi.org/10.1083/jcb.200407078

Kölzer, M., N. Werth, and K. Sandhoff. 2004. Interactions of acid sphingomyelinase and lipid bilayers in the presence of the tricyclic antidepressant desipramine. *FEBS Lett.* 559:96–98. http://dx.doi.org/10.1016/S0014-5793(04)00033-X

Liu, C., H. Miller, G. Orlowski, H. Hang, A. Upadhyaya, and W. Song. 2012. Actin reorganization is required for the formation of polarized B cell receptor signalosomes in response to both soluble and membrane-associated antigens. *J. Immunol.* 188:3237–3246. http://dx.doi.org/10.4049/jimmunol.1103065

Los, F.C., T.M. Randis, R.V. Aroian, and A.J. Ratner. 2013. Role of pore-forming toxins in bacterial infectious diseases. *Microbiol. Mol. Biol. Rev.* 77:173–207. http://dx.doi.org/10.1128/MMBR.00052-12

Mayor, S., and R.E. Pagano. 2007. Pathways of clathrin-independent endocytosis. *Nat. Rev. Mol. Cell Biol.* 8:603–612. http://dx.doi.org/10.1038/nrm2216

McNeil, P.L., and S. Ito. 1989. Gastrointestinal cell plasma membrane wounding and resealing in vivo. *Gastroenterology.* 96:1238–1248.

McNeil, P.L., and S. Ito. 1990. Molecular traffic through plasma membrane disruptions of cells in vivo. *J. Cell Sci.* 96:549–556.

McNeil, P.L., and R. Khakee. 1992. Disruptions of muscle fiber plasma membranes. Role in exercise-induced damage. *Am. J. Pathol.* 140:1097–1109.

Medina, F.A., T.M. Williams, F. Sotgia, H.B. Tanowitz, and M.P. Lisanti. 2006. A novel role for caveolin-1 in B lymphocyte function and the development of thymus-independent immune responses. *Cell Cycle.* 5:1865–1871. http://dx.doi.org/10.4161/cc.5.16.3132

Monroe, J.G., and J.C. Cambier. 1983. Sorting of B lymphoblasts based upon cell diameter provides cell populations enriched in different stages of cell cycle. *J. Immunol. Methods.* 63:45–56. http://dx.doi.org/10.1016/0022-1759(83)90208-9

Nabi, I.R., and P.U. Le. 2003. Caveolae/raft-dependent endocytosis. *J. Cell Biol.* 161:673–677. http://dx.doi.org/10.1083/jcb.200302028

Natkanski, E., W.Y. Lee, B. Mistry, A. Casal, J.E. Molloy, and P. Tolar. 2013. B cells use mechanical energy to discriminate antigen affinities. *Science.* 340:1587–1590. http://dx.doi.org/10.1126/science.1237572

Okada, T., M.J. Miller, I. Parker, M.F. Krummel, M. Neighbors, S.B. Hartley, A. O'Garra, M.D. Cahalan, and J.G. Cyster. 2005. Antigen-engaged B cells undergo chemotaxis toward the T zone and form motile conjugates with helper T cells. *PLoS Biol.* 3:e150. http://dx.doi.org/10.1371/journal.pbio.0030150

Parton, R.G., and K. Simons. 2007. The multiple faces of caveolae. *Nat. Rev. Mol. Cell Biol.* 8:185–194. http://dx.doi.org/10.1038/nrm2122

Pereira, J.P., L.M. Kelly, and J.G. Cyster. 2010. Finding the right niche: B-cell migration in the early phases of T-dependent antibody responses. *Int. Immunol.* 22:413–419. http://dx.doi.org/10.1093/intimm/dxq047

Pierce, S.K. 2002. Lipid rafts and B-cell activation. *Nat. Rev. Immunol.* 2:96–105. http://dx.doi.org/10.1038/nri726

Quah, B.J., V.P. Barlow, V. McPhun, K.I. Matthaei, M.D. Hulett, and C.R. Parish. 2008. Bystander B cells rapidly acquire antigen receptors from activated B cells by membrane transfer. *Proc. Natl. Acad. Sci. USA.* 105:4259–4264 (published erratum appears in *Proc. Natl. Acad. Sci. USA*. 2009. 106:14734). http://dx.doi.org/10.1073/pnas.0800259105

Reddy, A., E.V. Caler, and N.W. Andrews. 2001. Plasma membrane repair is mediated by Ca(2+)-regulated exocytosis of lysosomes. *Cell.* 106:157–169. http://dx.doi.org/10.1016/S0092-8674(01)00421-4

Rodríguez, A., P. Webster, J. Ortego, and N.W. Andrews. 1997. Lysosomes behave as Ca2+-regulated exocytic vesicles in fibroblasts and epithelial cells. *J. Cell Biol.* 137:93–104. http://dx.doi.org/10.1083/jcb.137.1.93

Rothstein, T.L. 1996. Signals and susceptibility to programmed death in b cells. *Curr. Opin. Immunol.* 8:362–371. http://dx.doi.org/10.1016/S0952-7915(96)80126-9

Singh, R.D., V. Puri, J.T. Valiyaveettil, D.L. Marks, R. Bittman, and R.E. Pagano. 2003. Selective caveolin-1-dependent endocytosis of glycosphingolipids. *Mol. Biol. Cell.* 14:3254–3265. http://dx.doi.org/10.1091/mbc.E02-12-0809

Sohn, H.W., P. Tolar, and S.K. Pierce. 2008. Membrane heterogeneities in the formation of B cell receptor-Lyn kinase microclusters and the immune synapse. *J. Cell Biol.* 182:367–379. http://dx.doi.org/10.1083/jcb.200802007

Song, W., C. Liu, M.K. Seeley-Fallen, H. Miller, C. Ketchum, and A. Upadhyaya. 2013. Actin-mediated feedback loops in B-cell receptor signaling. *Immunol. Rev.* 256:177–189. http://dx.doi.org/10.1111/imr.12113

Steinhardt, R.A., G. Bi, and J.M. Alderton. 1994. Cell membrane resealing by a vesicular mechanism similar to neurotransmitter release. *Science.* 263:390–393. http://dx.doi.org/10.1126/science.7904084

Stoddart, A., M.L. Dykstra, B.K. Brown, W. Song, S.K. Pierce, and F.M. Brodsky. 2002. Lipid rafts unite signaling cascades with clathrin to regulate BCR internalization. *Immunity.* 17:451–462. http://dx.doi.org/10.1016/S1074-7613(02)00416-8

Stoddart, A., A.P. Jackson, and F.M. Brodsky. 2005. Plasticity of B cell receptor internalization upon conditional depletion of clathrin. *Mol. Biol. Cell.* 16:2339–2348. http://dx.doi.org/10.1091/mbc.E05-01-0025

Tam, C., V. Idone, C. Devlin, M.C. Fernandes, A. Flannery, X. He, E. Schuchman, I. Tabas, and N.W. Andrews. 2010. Exocytosis of acid sphingomyelinase by wounded cells promotes endocytosis and plasma membrane repair. *J. Cell Biol.* 189:1027–1038. http://dx.doi.org/10.1083/jcb.201003053

Tam, C., A.R. Flannery, and N. Andrews. 2013. Live imaging assay for assessing the roles of Ca2+ and sphingomyelinase in the repair of pore-forming toxin wounds. *J. Vis. Exp.* 78:e50531.

Thyagarajan, R., N. Arunkumar, and W. Song. 2003. Polyvalent antigens stabilize B cell antigen receptor surface signaling microdomains. *J. Immunol.* 170:6099–6106. http://dx.doi.org/10.4049/jimmunol.170.12.6099

Tolar, P., H.W. Sohn, W. Liu, and S.K. Pierce. 2009. The molecular assembly and organization of signaling active B-cell receptor oligomers. *Immunol. Rev.* 232:34–41. http://dx.doi.org/10.1111/j.1600-065X.2009.00833.x

Tomassian, T., L.A. Humphries, S.D. Liu, O. Silva, D.G. Brooks, and M.C. Miceli. 2011. Caveolin-1 orchestrates TCR synaptic polarity, signal specificity, and function in CD8 T cells. *J. Immunol.* 187:2993–3002. http://dx.doi.org/10.4049/jimmunol.1101447

Torgersen, M.L., G. Skretting, B. van Deurs, and K. Sandvig. 2001. Internalization of cholera toxin by different endocytic mechanisms. *J. Cell Sci.* 114:3737–3747.

Trajkovic, K., C. Hsu, S. Chiantia, L. Rajendran, D. Wenzel, F. Wieland, P. Schwille, B. Brügger, and M. Simons. 2008. Ceramide triggers budding of exosome vesicles into multivesicular endosomes. *Science.* 319:1244–1247. http://dx.doi.org/10.1126/science.1153124

Wurster, A.L., V.L. Rodgers, M.F. White, T.L. Rothstein, and M.J. Grusby. 2002. Interleukin-4-mediated protection of primary B cells from apoptosis through Stat6-dependent up-regulation of Bcl-xL. *J. Biol. Chem.* 277:27169–27175. http://dx.doi.org/10.1074/jbc.M201207200

Xu, M., M. Xia, X.X. Li, W.Q. Han, K.M. Boini, F. Zhang, Y. Zhang, J.K. Ritter, and P.L. Li. 2012. Requirement of translocated lysosomal V1 H(+)-ATPase for activation of membrane acid sphingomyelinase and raft clustering in coronary endothelial cells. *Mol. Biol. Cell.* 23:1546–1557. http://dx.doi.org/10.1091/mbc.E11-09-0821

Yuseff, M.-I., P. Pierobon, A. Reversat, and A.-M. Lennon-Duménil. 2013. How B cells capture, process and present antigens: a crucial role for cell polarity. *Nat. Rev. Immunol.* 13:475–486. http://dx.doi.org/10.1038/nri3469